Theory of conduction band dispersion in dilute $B_xGa_{1-x}As$ alloys

A. Lindsay and E. P. O'Reilly
Tyndall National Institute, Lee Maltings, Prospect Row, Cork, Ireland
(Received 13 June 2007; published 30 August 2007)

The conduction band structure of $B_xGa_{1-x}As$ has a near-linear blueshift of the energy gap, which can be described using the virtual crystal approximation, but a dramatic increase in the band edge effective mass m_e^* at low B composition, similar to that observed in GaN_xAs_{1-x}. We use a tight-binding model to show that isolated B atoms have little effect either on the band gap or lowest conduction band dispersion in $B_xGa_{1-x}As$. In contrast, B pairs and clusters introduce defect levels close to the conduction band edge, which, through a weak band-anticrossing interaction, significantly reduce the band dispersion in and around the Γ point, thus accounting for the strong increase in m_e^* and reduction in mobility observed in these alloys.

DOI: 10.1103/PhysRevB.76.075210 PACS number(s): 72.20.Dp, 72.10.Fk

I. INTRODUCTION

There has been considerable interest in extreme semiconductor alloys in recent years, both from a fundamental perspective and also because of their significant potential device applications.[1] The electronic structure of a conventional alloy, such as $Al_xGa_{1-x}As$, is well described using the virtual crystal approximation (VCA), which treats the group III atoms in this alloy as if they were all replaced by a virtual group III atom whose properties are an average of those of gallium (Ga) and aluminum (Al). In contrast, the difference in electronegativity and size between arsenic (As) and nitrogen (N) is so large that when we replace an As atom by N in GaAs, the N atom introduces a resonant defect level above the GaAs conduction band edge.[2] Many aspects of the band structure of GaN_xAs_{1-x}, including the strong band-gap bowing, are then well described using a band-anticrossing (BAC) model, which explains the evolution of the band structure in terms of interactions between the localized N-related states and the host matrix conduction band states.[3]

The semiconductor alloy $B_xGa_{1-x}As$ provides an interesting case of a material whose properties are intermediate between those of a conventional and an extreme semiconductor alloy. The difference in atom size between boron (B) and Ga is considerably greater than in conventional alloys, suggesting that it might display similar extreme properties to those observed in GaN_xAs_{1-x}. In practice, the experimentally measured variation of energy gap with composition in $B_xGa_{1-x}As$ is well described using the VCA,[4,5] in agreement with *ab initio* calculations carried out on ordered BGaAs supercells containing up to 64 atoms.[6] In contrast, recent experiments on $B_{0.03}In_{0.06}Ga_{0.91}As$ using far-infrared magneto-optic ellipsometry have shown a 44% increase in electron effective mass over that expected for $In_{0.06}Ga_{0.94}As$,[7] considerably larger than that predicted using the VCA, with a further increase in mass measured with increasing carrier concentration. The recently measured electron mobility of 800 $cm^2\,(V\,s)^{-1}$ in a BInGaAs sample at ambient pressure[8] is intermediate between that of a conventional alloy and the very low values [of order of 100–300 $cm^2\,(V\,s)^{-1}$] observed in GaNAs alloys,[9] with the measured mobility in the BGaAs case decreasing rapidly with increasing hydrostatic pressure to ~100 $cm^2\,(V\,s)^{-1}$ at 14 kbar, similar to the observed values in GaNAs.[8] Hence, the electronic properties of BGaAs are intermediate between those of conventional and extreme alloys, with some of the measured properties as expected for conventional alloys, while others resemble more closely those of an extreme alloy.

We investigate here the cause of the unusual electronic properties of dilute $B_xGa_{1-x}As$ alloys. The strong reduction in energy gap observed with increasing N composition x in GaN_xAs_{1-x} can be explained in terms of the BAC interaction between the GaAs host conduction band edge and a higher lying band of states associated with isolated N atoms, where the substitutional N atoms only have As second nearest neighbors. A random GaNAs alloy contains not only isolated N atoms but also N-N pairs, where a Ga atom has two N neighbors, and larger clusters of N atoms, with the proportion of pairs and larger clusters increasing rapidly with increasing composition x. We have shown previously that the anomalously large electron mass, low mobility, and anomalous electron gyromagnetic ratio observed in GaN_xAs_{1-x} are due to the distribution of energy states associated with the N-N pair and cluster states.[9–12] We extend our previous investigations here to consider BGaAs alloys. We show that, due to the large size and electronegativity difference between B and Ga, isolated B atoms, and B-B pair and cluster states, all introduce resonant defect levels above the conduction band edge of BGaAs. However, the BAC interaction is much reduced between these states and the conduction band edge.

We present here the band structure of $B_xGa_{1-x}As$, GaN_xAs_{1-x} and four conventional GaAs alloys for low alloy composition ($x=2.6\%$) using a tight-binding model that includes the effects of lattice distortion due to the size difference between the host and substitutional atoms. The details of the tight-binding method used are presented in the next section. We then present and discuss the results of band structure calculations on 1000-atom supercells. These calculations confirm the VCA approach for $(In,Al)_xGa_{1-x}As$ and for $Ga(P,Sb)_xAs_{1-x}$ and previous results for GaNAs. $B_mGa_{500-m}As_{500}$ supercell calculations (with $m=13$ and $x=2.6\%$) show that B introduces a highly localized A_1 state in the conduction band, which lies ~300 meV above the GaAs conduction band edge (CBE), and that B-B pairs and/or related clusters of B atoms give rise to localized impurity levels which lie close to the BGaAs CBE. In all cases, their

TABLE I. Energies (in eV) of the sp^3s^* tight-binding parameters used for bulk GaAs, zinc-blende GaN, and BAs for $T=0$ K. The zero of energy is set at the valence band maximum of GaAs. The valance band maximum of GaN and BAs is assumed to lie below that of GaAs by 2.28 and 0.19 eV, respectively (Refs. 14 and 6).

	GaAs	GaN	BAs
E_s^a	−8.8128	−14.8931	−7.8945
E_s^c	−3.5355	−4.0862	−4.1428
E_p^a	1.0414	0.4397	0.9535
E_p^c	3.6686	6.3003	1.9265
$E_{s^*}^a$	12.9297	18.1200	17.9226
$E_{s^*}^c$	12.9297	18.1200	17.9226
$ss\sigma$	−2.0045	−2.5523	−2.9601
$s_ap_c\sigma$	1.8847	1.5484	1.9653
$s_cp_a\sigma$	2.3668	2.8959	2.1895
$pp\sigma$	2.9811	5.0530	3.2285
$pp\pi$	−0.7576	−0.7150	−1.0309
$s_a^*p_c\sigma$	2.6615	1.8502	3.1433
$s_c^*p_a\sigma$	2.7133	3.8508	3.8272
$s_a^*s_c\sigma$	0.4674	0.5852	0.6546
$s_c^*s_a\sigma$	0.6299	1.1181	0.8824
$s^*s^*\sigma$	1.3730	2.1674	1.9234
$s_ax_{a'}(0,1,1)$	0.0000	−0.7040	0.0000

interaction with the GaAs CBE is close to an order of magnitude smaller than that calculated for N, explaining their weak effect on the conduction band energy. However, due to the close proximity of the pair and cluster levels to the CBE, there can be a significant reduction in the CBE dispersion due to this weak anticrossing effect. This reduced BAC interaction and the distribution of B resonant defect levels can then account for the behavior both of the energy gap and of the electron effective mass and mobility in BGaAs.

II. DETAILS OF TIGHT-BINDING MODEL

We use an accurate sp^3s^* nearest-neighbor tight-binding Hamiltonian to investigate the electronic structure of the different alloys. The interatomic parameters are allowed to vary with bond length, while the magnitude of the on-site parameters depends explicitly on the overall neighbor environment. The calculations are undertaken on 1000-atom supercells in which all atomic positions have been relaxed using the GULP molecular relaxation package[13] and a parametrized valence force field (VFF) model while using Végard's law to constrain the average lattice constant as $a(x)=xa_{\mathrm{Ga}}Y/X_{\mathrm{As}}+(1-x)a_{\mathrm{GaAs}}$. The calculated relaxed bond lengths are in good agreement with those obtained by Bellaiche *et al.*,[14] who have shown that relaxations calculated using the VFF approach agree well with those determined from *ab initio* calculations. The on-site orbital energies for a given atom are determined by taking an average of the values from the binary compounds formed by that atom and its four nearest neighbors, with a further minor adjustment due to changes in the next-nearest neighbor shell. The interatomic interaction energies are taken to vary with bond length d as $(d_0/d)^n$, where d_0 is the equilibrium bond length in the equivalent binary compound and n is a scaling exponent whose magnitude depends on the type of interaction being considered. The effects of changes in bond angle are taken into account through the two-center integral expressions of Slater and Koster.[15] The scaling indices are determined by fitting the bond length dependence of the GaAs, GaN, and BAs nearest-neighbor interaction parameters to a range of hydrostatic deformation potentials.[16,17] This was also carried out for the other compounds involved. The self-energy and interatomic interaction parameters used in the model are mainly taken from Vogl *et al.*[18] The parameters for GaN and BAs were derived by fitting to pseudopotential band structure calculations for the zinc-blende structure.[6,14] The GaAs parameters were modified from those of Vogl *et al.* to give an accurate fit to the standard values of the CBE Γ, X, and L, energies in GaAs. The parameters of Vogl *et al.* give a Γ-L separation of 140 meV, compared to the measured low-temperature separation of 330 meV. We have found previously that the calculated energies of N resonant defect levels in GaN_xAs_{1-x} are very sensitive to the magnitude of the Γ-L splitting used in the calculation.[19] A similar refitting of the parameters was also made for AlAs, InAs, GaP, and GaSb. The Hamiltonian which we use also includes nonzero interactions between s and s^* orbitals to give an accurate fit to the conduction band effective mass at Γ in each of the binary compounds considered.

TABLE II. Calculated indices $n_{\alpha\beta}$ to describe the distance dependence of the interatomic interactions between orbitals α and β on neighboring atoms.

$n_{\alpha\beta}$	GaAs	GaN	BAs
$ss\sigma$	3.21	2.69	3.85
$s_ap_c\sigma$	4.20	4.24	2.00
$s_cp_a\sigma$	4.20	3.56	2.00
$pp\sigma$	3.20	2.09	3.00
$pp\pi$	4.24	3.72	4.02
$s_a^*p_c\sigma$	3.80	3.71	2.70
$s_c^*p_a\sigma$	6.90	6.45	2.90
$s_a^*s_c\sigma$	0.00	3.19	0.00
$s_c^*s_a\sigma$	0.00	2.60	0.00

Tables I and II list the tight-binding parameters used for GaAs, GaN, and BAs. Table I lists the parameters for the zinc-blende binary compounds, while Table II shows the scaling exponent n used to describe the variation of the interatomic matrix elements with bond length. The calculated values of the conduction band mass and of various energy gaps and deformation potentials are then compared with values from the literature in Table III.

III. RESULTS AND DISCUSSION

Full tight-binding calculations were carried out to compare the conduction band structure of GaAs and of six ter-

TABLE III. Calculated band-gap energies E, hydrostatic deformation potentials a, and Γ_{1c} effective mass $m^*(\Gamma_{1c})$ (in units of m_0) using the parameters in Tables I and II (values with no superscript). Results from other sources are given for comparison.

	GaAs	GaN	BAs
		E (eV)	
$\Gamma_{15v} \rightarrow \Gamma_{1c}$	1.515, 1.519[a]	3.22, 3.37[b]	4.59, 4.57[c]
$\Gamma_{15v} \rightarrow L_{1c}$	1.861, 1.85[a]	5.65, 5.88[b]	2.66, 2.60[c]
$\Gamma_{15v} \rightarrow X_{1c}$	1.976, 1.98[a]	4.59, 4.59[b]	1.28, 1.27[c]
$\Gamma_{15v} \rightarrow \Delta_{\min}$			0.99(0.83,0,0), 1.06(0.80,0,0)[d]
		a (eV)	
$\Gamma_{15v} \rightarrow \Gamma_{1c}$	−8.39, −8.33[e]	−7.00, −6.98[b]	−12.42, −12.35[d]
$\Gamma_{15v} \rightarrow L_{1c}$	−4.25, −4.13[a]	−4.50, −4.78[b]	−6.47, −5.79[d]
$\Gamma_{15v} \rightarrow X_{1c}$	1.44, 1.37[a]	0.38, 0.42[b]	1.23, 1.26[d]
Γ_{15v}	1.16, 1.16[e]	2.0, 2.0[f]	0.58, 0.57[d]
$m^*(\Gamma_{1c})$	0.0672, 0.0670[a]	0.17, 0.13[b] 0.15[g]	0.23

[a]References 20 and 21.
[b]Reference 14.
[c]Reference 6.
[d]Reference 17.
[e]Reference 22.
[f]Reference 23.
[g]Reference 24.

nary GaAs alloys. In each case, we have taken a 1000-atom GaAs supercell and replaced the same 13 Ga (or As) atoms by N, B, P, Sb, Al, or In to investigate the band structure of $X_xGa_{1-x}As$ and GaY_xAs_{1-x} (X=B,Al,In and Y=N,P,Sb) for an alloy composition of x=2.6%. In the first series of structures, we introduced a random distribution of alloy atoms but with the constraint that the structure only includes isolated alloy atoms, with no anion (cation) atom having two or more X (Y) atoms as nearest neighbors. We then took a second series of structures in which we started with the same distribution of alloy atoms as in the first case but then moved two of the atoms to give an arrangement of nine isolated alloy atoms and two alloy pairs, where a pair is formed when two alloy atoms share a common nearest-neighbor host atom. This is close to the proportion of pairs and isolated alloy atoms expected in a random alloy around this composition. There is in addition, a smaller fraction of larger clusters in a random alloy, which is omitted in the present model structure.

Throughout the following discussion, we focus only on the conduction band structure, because in all the cases considered (N and B included), we calculate that the upper valance bands remain largely unperturbed.

Figure 1(a) shows the conduction band dispersion of a 1000-atom GaAs supercell, calculated along the k_z direction, while Figs. 1(b)–1(e) show the calculated band dispersion of the conventional alloys (X=Al,In and Y=Sb,P, respectively). The dispersion is plotted in Figs. 1(b)–1(e), both for the structure with only isolated atoms (dotted lines) and also for the structure with two pairs (solid lines) present. It is, in general, almost impossible to distinguish the two sets of data. Figures 1(b)–1(e) show that the dispersion of the lowest conduction band is well described for each of these alloys by the VCA; the lowest conduction band is similar to that of GaAs, and there are no unusual features in the dispersion of this band up to the Brillouin zone edge of the 1000-atom supercell, even with the inclusion of pairs (solid lines). This is further confirmed in Fig. 2 which compares the calculated conduction band edge effective mass for several alloys with that predicted using the VCA. The open data points show the calculated mass for structures containing only isolated alloy atoms, while the solid data points are for structures containing both isolated and pair impurities. It is impossible on the scale of Fig. 2 to distinguish between the calculated mass with and without the inclusion of alloy atom pairs in the calculations for the four conventional alloys of Fig. 1. The calculated mass for each of these four alloys is also in excellent agreement with the values predicted using the VCA (solid line in Fig. 2).

Turning our attention now to GaNAs and to Fig. 3(a) for the first case with isolated N atoms only, we observe both a dramatic reduction in the CBE energy of around 0.35 eV and also a marked reduction in the dispersion. A group of 12 new states is introduced between 1.6–1.8 eV at Γ. These have been shown to be 12 different combinations of the impurity states associated with the 13 isolated N atoms.[25] We can extract from the calculations a 13th state formed from a symmetric combination of the isolated impurity states, which interacts strongly with the CBE to give a N-related resonant state in the conduction band at ~2 eV. This higher energy N-related state can be identified with the E_+ level observed in GaNAs.[3] At this energy, the E_+ level is strongly degenerate with the host density of states and so is spread over many close lying conduction levels.[25] The two-level BAC model can successfully fit both the band edge energy and also the lowest conduction band dispersion in Fig. 3(a). In contrast to the conventional alloys, the band dispersion shown in Fig. 3(b) for a GaNAs supercell including two N-N pairs is markedly different to that in Fig. 3(a). There are now two zone center states (at about 1.46 and 1.54 eV) associated with the

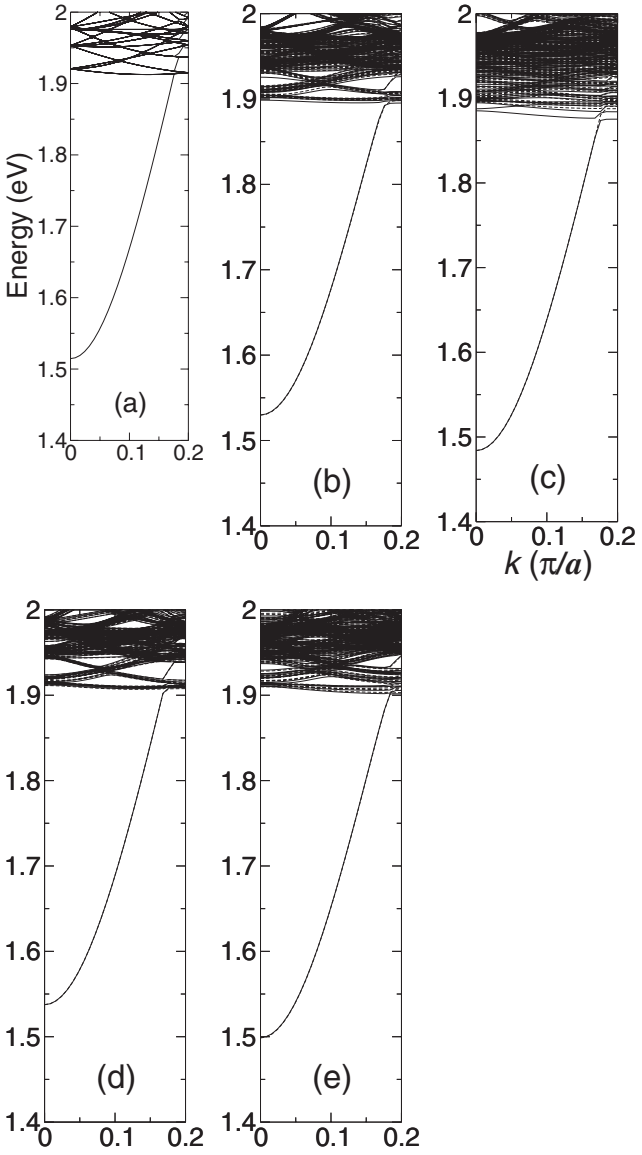

FIG. 1. Calculated conduction band structure of (a) $Ga_{500}As_{500}$, and the 2.6% alloys $X_{13}Ga_{487}As_{500}$ and $Ga_{500}Y_{13}As_{487}$ containing only isolated (dotted lines) and both isolated and pair (solid lines) X or Y atoms, with (b) X=Al, (c) X=In, (d) Y=P, and (e) Y=Sb. The band dispersion is calculated along the k_z direction in units of π/a, where a is the appropriate Végard lattice constant.

two N nearest-neighbor pairs. These states have a strong anticrossing interaction with the lowest conduction band, shifting the band edge energy down by about ~30 meV and further increasing the zone center effective mass, as indicated in Fig. 2. We note that at this composition, the N-N levels lie too far above the CBE to have a dramatic effect on the mass, because the strong anticrossing with the isolated N states has pushed the CBE energy about 300 meV below the N-N pair state energies. We have shown previously that the presence of N-related states close to the CBE significantly enhances the CBE effective mass. We found in ultralarge supercells with x between 0.1% and 0.2% that the pair states lie much closer to the CBE and so can strongly hybridize with it. This hybridization reduced the conduction band Γ character significantly below the BAC value, leading to a significant increase in mass.[10] A similar mass enhancement was also obtained for larger values of x using a statistical distribution of N atoms where the CBE lies close in energy to states associated with larger N complexes. Figure 3(c) illustrates the same effect for the 1000-atom supercells considered here, showing how the band structure of Fig. 3(b) changes under the applied hydrostatic pressure of 22 kbar. Figure 2 shows that the CBE mass increases by 26% in Fig. 3(c) compared to Fig. 3(b). This confirms how the effective mass depends on the separation between the pair or cluster levels and the CBE, and it also emphasizes the overall importance of disorder in GaNAs.

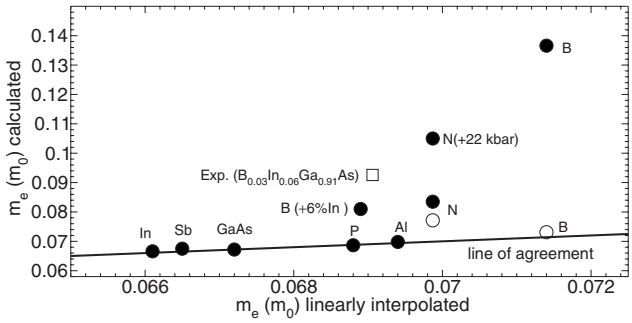

FIG. 2. Electron effective mass directly obtained from lowest conduction band of each of the various XGaAs and GaYAs alloys plotted against that predicted by VCA (X/Y indicated for each data point). Open points: structures containing only isolated impurities. Closed points: structures containing both isolated and pair impurities. Points lying on the line indicate exact agreement between the extracted and VCA values.

Figure 4(a) shows the band structure of a supercell containing 13 isolated B atoms. We calculate a small blueshift in the band gap, consistent with that measured experimentally.[4] The calculated electron effective mass is also close to that predicted using the virtual crystal approximation (see Fig. 2). Nevertheless, there are a large number of B-related defect states above the conduction band edge. We find 39 levels between 1.7 and 1.8 eV, associated with highly localized B states of T_d-type symmetry (three per B atom). Above this is a further group of 13 highly localized B states with A_1 symmetry (one per B atom). In BGaAs, contrary to GaNAs, we calculate the T_d levels of the isolated impurity to lie below the A_1 levels. The T_d states do not interact with the CBE, for symmetry reasons, while the A_1 levels have a much weaker interaction and effect than in GaNAs, due to the different host state character of the A_1 states in BGaAs compared to GaNAs, as discussed further in Ref. 26. Turning to Fig. 4(b) and the supercell containing nine isolated B atoms and two pairs, we see a dramatic effect near the conduction band minimum, with the introduction of two new levels associated with the two B-B pairs, which lie just above the CBE. These states have a small interaction through which they strongly hybridize with the CBE at Γ, an effect which more than doubles the calculated band edge effective mass (see Fig. 2). This increase is in good agreement with that measured for higher carrier concentrations in n-doped dilute boride alloys.[7] The interaction between the pair levels and the CBE

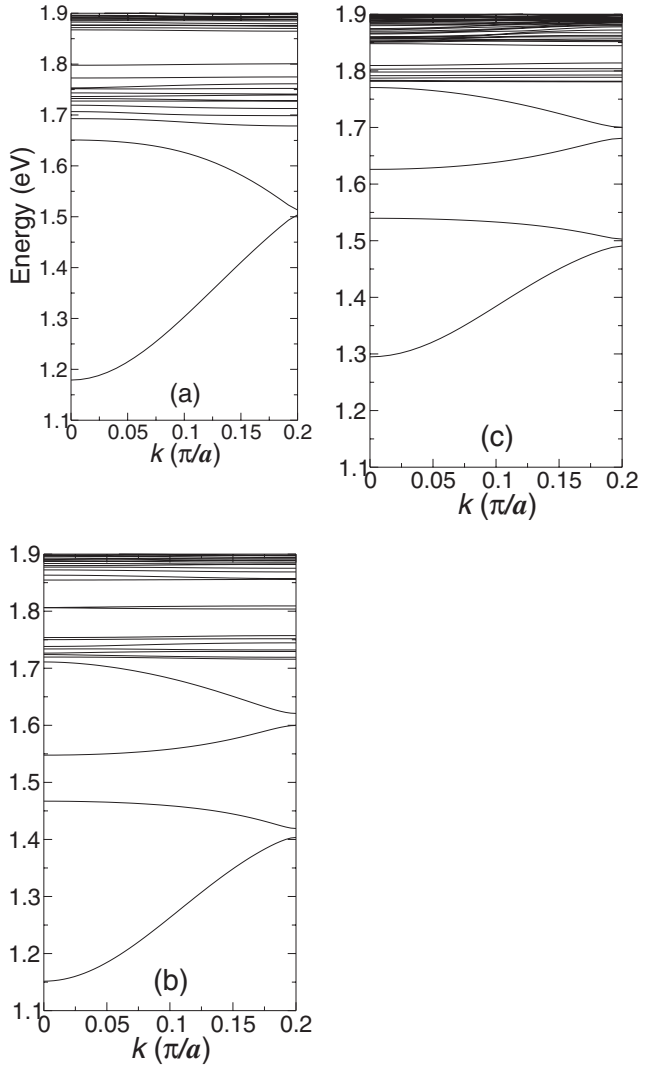

FIG. 3. Calculated band structure of a $Ga_{500}N_{13}As_{487}$ supercell (2.6% alloy composition) containing (a) 13 isolated N atoms, (b) nine isolated N atoms and two N-N pairs, and (c) the same as (b) for the applied hydrostatic pressure of 22 kbar. The band dispersion is calculated along the k_z direction in units of π/a, where a is the alloy lattice constant.

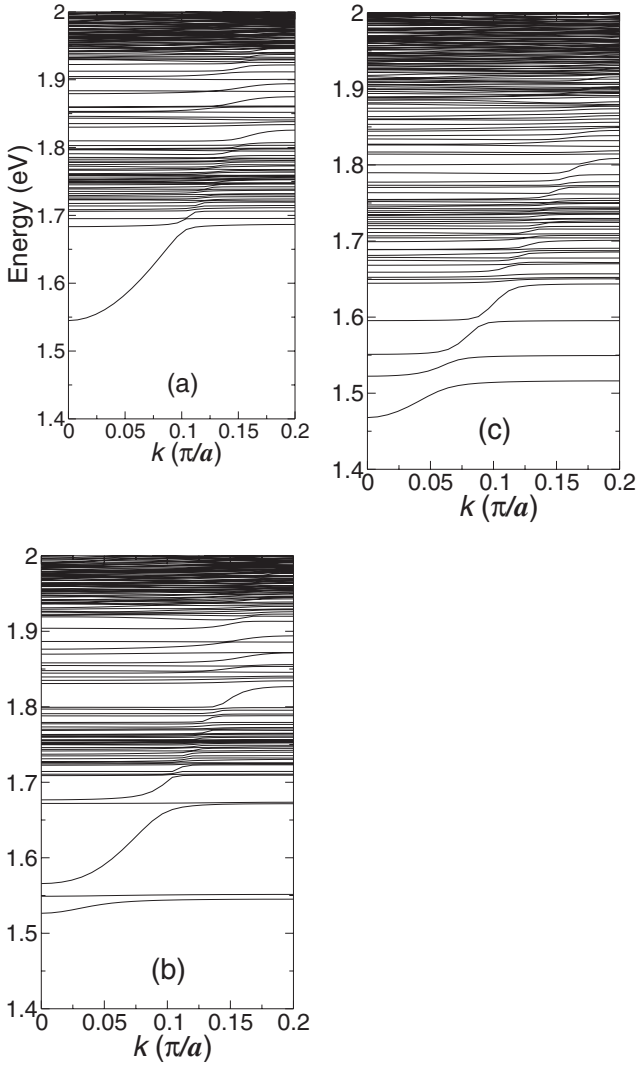

FIG. 4. Calculated band structure of a $B_{13}Ga_{487}As_{500}$ supercell (2.6% B alloy) containing (a) 13 isolated B atoms, (b) nine isolated B atoms and two B-B pairs, and (c) the alloy $B_{13}In_{30}Ga_{457}As_{500}$ with nine isolated B atoms, two B-B pairs, and 30 randomly distributed In atoms replacing Ga. The band dispersion is calculated along the k_z direction in units of π/a, where a is the appropriate alloy lattice constant.

also lowers the band edge by around 20 meV. If we move the band edge away from the pair levels, e.g., by introducing a number of In atoms into the supercell, as shown in Fig. 4(c), we see a strong recovery in the dispersion near the conduction band minimum. We calculate that shifting the band edge down by around 50 meV reduces by more than a factor of 2 the effect of these levels on the band edge mass. The calculated band edge mass for the $B_{13}In_{30}Ga_{457}As_{500}$ supercell of Fig. 4(c) is around 30% larger than the VCA value for this alloy. This is comparable with the 44% increase obtained for a $B_{0.027}In_{0.06}Ga_{0.913}As$ alloy at low electron concentrations.[7] We note that many of the B defect levels shift down in energy when we include In. One level in Fig. 4(c) is at an energy close to that of the two B-B pair levels. This state is mostly p-like in nature. It is predominantly localized on one of the isolated B atoms for which four of the 12 second nearest neighbors are In atoms. Because In is larger in size than Ga, when In replaces any of the 12 second neighbor Ga atoms, it allows the BAs bond to relax more toward the BAs equilibrium bond length. This has the effect here of lowering the energy of one of the p-like T_d states associated with that B atom.

The band dispersion presented in Fig. 4 is consistent with recently reported measurements of the mobility of BGa(In)As both at ambient pressure and under applied hydrostatic pressure.[7] We have shown that the mobility is strongly limited in GaN_xAs_{1-x} alloys due to resonant scattering by N-related defect levels, with such resonant scattering explaining the typical mobility values of 100–300 $cm^2\,(V\,s)^{-1}$ observed in GaNAs alloys.[9] We expect that the B-related resonant defect levels above the CBE in BGaAs will act as weaker resonant scattering centers compared to N in GaNAs, consistent with a measured mobility of order of

800 cm^2 $(V\ s)^{-1}$ at ambient pressure. The resonant scattering rate will then increase with applied hydrostatic pressure, as the resonant scattering levels approach the CBE, consistent with the observed decrease in mobility with increasing hydrostatic pressure.

IV. CONCLUSIONS

In summary, the semiconductor alloy $B_xGa_{1-x}As$ provides an interesting case of a material whose properties are different both from those of a conventional semiconductor alloy and also from other extreme semiconductor alloys such as GaNAs. Neither the virtual crystal approximation nor the band-anticrossing model can successfully fit both the observed change in band gap and effective mass with increasing x. We have shown here that this unusual behavior can be explained through a detailed analysis of boron-related resonant defect states in BGaAs. Tight-binding calculations show that isolated B atoms have little effect either on the band gap or lowest conduction band dispersion in BGaAs. In contrast, B pairs and clusters introduce a series of defect levels close to the conduction band edge which, through a weak band-anticrossing interaction, significantly reduce the band dispersion in and around the Γ point. Thus, we must include hybridization between the GaAs host band states and pair or cluster defect levels lying close to the band edge to account for the strong increase in m_e^* and reduction in mobility observed in these alloys. We conclude that the two-level band-anticrossing model is not appropriate in describing the energy gap in BGaAs but that the corrections previously introduced to account for the large increase in m_e^* in GaNAs are also required to explain m_e^* in BGaAs.

ACKNOWLEDGMENTS

This work is supported by the Science Foundation Ireland. We thank P. J. Klar for useful discussions.

[1] For a review, see *Physics and Applications of Dilute Nitrides*, edited by I. A. Buyanova and W. M. Chen (Taylor & Francis, New York, 2004).
[2] D. J. Wolford, J. A. Bradley, K. Fry, and J. Thompson, *Proceedings of the 17th International Conference on the Physics of Semiconductors* (Springer, New York, 1984), p. 627.
[3] W. Shan, W. Walukiewicz, J. W. Ager III, E. E. Haller, J. F. Geisz, D. J. Friedman, J. M. Olson, and S. R. Kurtz, Phys. Rev. Lett. **82**, 1221 (1999).
[4] G. Leibiger, V. Gottschalch, V. Riede, M. Schubert, J. N. Hilfiker, and T. E. Tiwald, Phys. Rev. B **67**, 195205 (2003).
[5] W. Shan, W. Walukiewicz, J. Wu, K. M. Yu, J. W. Ager III, S. X. Li, E. E. Haller, J. F. Geisz, D. J. Friedman, and S. R. Kurtz, J. Appl. Phys. **93**, 2696 (2003).
[6] G. L. W. Hart and A. Zunger, Phys. Rev. B **62**, 13522 (2000).
[7] T. Hofmann, M. Schubert, C. von Middendorff, G. Leibiger, V. Gotschalch, C. M. Herzinger, A. Lindsay, and E. P. O'Reilly, in *Physics of Semiconductors: 27th International Conference on the Physics of Semiconductors*, edited by J. Menédez and C. G. Van de Walle, AIP Conf. Proc. No. 772 (AIP, New York, 2005), pp. 455–456.
[8] J. Teubert, P. J. Klar, W. Heimbrodt, V. Gottschalch, A. Lindsay, and E. P. O'Reilly, Phys. Status Solidi B **244**, 431 (2007).
[9] S. Fahy, A. Lindsay, H. Ouerdane, and E. P. O'Reilly, Phys. Rev. B **74**, 035203 (2006).
[10] A. Lindsay and E. P. O'Reilly, Phys. Rev. Lett. **93**, 196402 (2004).
[11] F. Masia, G. Pettinari, A. Polimeni, M. Felici, A. Miriametro, M. Capizzi, A. Lindsay, S. B. Healy, E. P. O'Reilly, A. Cristofoli, G. Bais, M. Piccin, S. Rubini, F. Martelli, A. Franciosi, P. J. Klar, K. Volz, and W. Stolz, Phys. Rev. B **73**, 073201 (2006).
[12] G. Pettinari, F. Masia, A. Polimeni, M. Felici, A. Frova, M. Capizzi, A. Lindsay, E. P. O'Reilly, P. J. Klar, W. Stolz, G. Bais, M. Piccin, S. Rubini, F. Martelli, and A. Franciosi, Phys. Rev. B **74**, 245202 (2006).
[13] J. Gale, J. Chem. Soc., Faraday Trans. **93**, 629 (1997).
[14] L. Bellaiche, S.-H. Wei, and A. Zunger, Phys. Rev. B **54**, 17568 (1996).
[15] J. C. Slater and G. F. Koster, Phys. Rev. **94**, 1498 (1954).
[16] E. P. O'Reilly, A. Lindsay, S. Tomić, and M. Kamal-Saadi, Semicond. Sci. Technol. **17**, 870 (2002).
[17] B. Bouhafs, H. Aourag, and M. Certier, J. Phys.: Condens. Matter **12**, 5655 (2000).
[18] P. Vogl, H. P. Hjalmarson, and J. D. Dow, J. Phys. Chem. Solids **44**, 365 (1983).
[19] A. Lindsay, Ph.D. thesis, University of Surrey, 2002.
[20] *Semiconductors: Group IV Elements and III-V Compounds*, edited by O. Madelung, Landolt-Börnstein, New Series, Group III, Vol. 17, Pt. A (Springer, Berlin, 1982).
[21] *Semiconductors: Intrinsic Properties of Group IV Elements and III-V, II-VI, and I-VII Compounds*, edited by O. Madelung, Landolt-Börnstein, New Series, Group III, Vol. 22, Pt. A (Springer, Berlin, 1987).
[22] C. G. Van de Walle, Phys. Rev. B **39**, 1871 (1989).
[23] C. G. Van de Walle and J. Neugebauer, Appl. Phys. Lett. **70**, 2577 (1997).
[24] M. Fanciulli, T. Lei, and T. D. Moustakas, Phys. Rev. B **48**, 15144 (1993).
[25] A. Lindsay and E. P. O'Reilly, Physica E (Amsterdam) **21**, 901 (2004).
[26] A. Lindsay and E. P. O'Reilly, Physica B **340-342**, 434 (2003).